BIOMECHANICAL REPORT

FOR THE

IAAF World Championships
LONDON 2017

High Jump Women's

Dr Gareth Nicholson and Dr Athanassios Bissas
Carnegie School of Sport

Stéphane Merlino
IAAF Project Leader

LEEDS BECKETT UNIVERSITY

IAAF™

Event Director Dr Gareth Nicholson		**Project Director** Dr Athanassios Bissas
	Project Coordinator Louise Sutton	
	Senior Technical Support	
Liam Gallagher	Aaron Thomas	Liam Thomas
Senior Research Officer Josh Walker	**Report Editor** Dr Catherine Tucker	**Analysis Support** Dr Lysander Pollitt
Logistics Dr Zoe Rutherford	**Calibration** Dr Brian Hanley	**Data Management** Nils Jongerius
	Technical Support	
Ashley Grindrod Joshua Rowe	Ruth O'Faolain	Lewis Lawton Joe Sails
	Data Analysts	
Dr Gareth Nicholson	Emily Gregg	Nils Jongerius
	Project Team	
Dr Tim Bennett	Mark Cooke Helen Gravestock	Dr Alex Dinsdale
Masalela Gaesenngwe	Mike Hopkinson	Parag Parelkar
Rachael Bradley Jamie French Philip McMorris William Shaw Dr Emily Williams	Amy Brightmore Callum Guest Maria van Mierlo James Webber Jessica Wilson Dr Stephen Zwolinsky	Helen Davey Ruan Jones Dr Ian Richards Jack Whiteside Lara Wilson
	External Coaching Consultant Denis Doyle	

Table of Contents

INTRODUCTION 1

METHODS 2

RESULTS 7

COACH'S COMMENTARY 27

CONTRIBUTORS 31

Figures

Figure 1. Camera locations for the women's high jump final (highlighted in green). 2

Figure 2. The calibration frame was constructed and filmed before and after the competition. 3

Figure 3. Action from the women's high jump final. 4

Figure 4. Key time-points at which the selected variables were obtained. C1-C4 denote foot contacts. 4

Figure 5. Partials heights of each athlete's CM during their best attempt. 7

Figure 6. Scatterplot showing the distance of the CM (peak height) relative to the cleared mark in the vertical and horizontal directions for each finalist. Minus values on the horizontal scale indicate area beyond the bar. 8

Figure 7. Contrasting bar clearance techniques of the medallists, with Lasitskene (top), Levchenko (middle) and Licwinko (bottom). 9

Figure 8. Percentage change in CM height during the last step for each of the finalists. 11

Figure 9. The vertical position of the CM during the approach for the gold medallist. 11

Figure 10. The horizontal velocity of each finalist at TD during the second, third and fourth (take-off) foot contacts. 12

Figure 11. Contrasting rear foot position during take-off TD for three of the finalists. 13

Figure 12. Overhead view of the CM path during the approach, take-off and airborne phase. Dashed lines depict the construction of the CM attack angles reported in Table 6. 14

Figure 13. Schematic representation of the step-to-bar angle for each foot contact relative to the next. 15

Figure 14. The overhead views of the paths of the CM during the approach and take-off for the finalists. Medallists are represented by solid lines. 16

Figure 15. Overhead views of the CM and foot path during the approach, take-off and airborne phases for the three medallists. 17

Figure 16. Length of the last three approach steps for each of the finalists. 18

Figure 17. The contrasting take-off distances of Jungfleisch (left) and Demireva (right). 19

Figure 18. Scatterplots showing the relationships between key variables. *r* values indicate correlation coefficients. 20

Figure 19. The top figure shows the range of motion between maximum knee flexion and the knee angle at take-off for each of the finalists. Bottom: Range of motion between maximum ankle flexion and the ankle angle at take-off for each of the finalists. 22

Figure 20. Top: Contact times for the final four ground contacts during the approach for each of the finalists. Bottom: Flight times for the final three steps before take-off (flight 3 precedes contact 4) for each of the finalists. 23

Figure 21. Top: Ratio of flight time to ground contact time during the final step. Bottom: relationship between the duration of knee flexion (during take-off) and the ratio of flight time to contact during the final step. 24

Figure 22. The percentage of time spent during knee flexion and extension during the final foot contact (take-off phase). 25

Figure 23. Example of body orientation at TD during the take-off phase for Licwinko. 26

Tables

Table 1. Definitions of mechanical and performance variables. 5

Table 2. Best mark attained for each of the finalists expressed relative to their previous bests (before the London World Championships). 7

Table 3. Partial heights of the CM (in metres and relative to each athlete's stature) along with the peak CM location, peak pelvis height and PPH diff for each finalist. 8

Table 4. The height (relative to stature) of the CM at contact two, three and four along with the change in height (% of stature) during the take-off phase, mean approach height (% stature) and the percentage lowering of the CM from penultimate to final TD (not relative to stature). 10

Table 5. The horizontal velocity of the CM at TD during each foot contact (fourth contact = take-off) and at TO of contact four. The change (%) in horizontal velocity during take-off (from TD to TO) is also displayed. 12

Table 6. CM attack angle at toe-off for the first, second, third and fourth foot contacts along with the percentage change in this angle from the first to the fourth foot contact. 14

Table 7. Step-to-bar angle between toe-off to toe-off of each respective foot contact along with the percentage change in these angles from one to the next (1-3 indicates the % change from the first to the final angle). 15

Table 8. The length of the last three approach steps along with the contact time of the take-off phase (CT) for the finalists. Step lengths are also expressed as a percentage of each athlete's standing height. 18

Table 9. The vertical (V_v) and resultant (V_r) velocity values at TD and TO during the take-off phase along with the velocity transfer, take-off angle and take-off distances. 19

Table 10. The knee angles at the instant of touchdown (TD) and toe-off (TO) during the penultimate foot contact for all finalists. Knee and ankle angles are also displayed at TD, TO and its lowest value during the final (take-off) contact. 21

Table 11. The time spent in knee flexion and extension during the penultimate and final foot contacts. 25

Table 12. The whole-body lean at touchdown and toe-off during the take-off phase and the trunk lean at touchdown for each of the finalists. 26

INTRODUCTION

The women's high jump final took place in favourable weather conditions on the penultimate day of the championships on August 12th. Leading up to the event, the reigning World Champion Maria Lasitskene was the favourite to retain her title. Lasitskene topped the outdoor season best list with a mark of 2.06 m. It was Ukraine's Yulia Levchenko who had come closest to Lasitskene's world lead in 2017 clearing a mark of 2.01 m in the London stadium only the month before. Although Poland's Kamila Licwinko and Ukraine's Levchenko went ahead of Lasitskene on the night with first-time clearances at 1.99 m, Lasitskene recovered to retain her title with a first-time clearance at 2.03 m. Having already sealed victory, Lasitskene failed to better her lifetime best with failed attempts at 2.08 m but it was Levchenko (2.01 m) and Licwinko (1.99 m) who produced personal and season's bests to claim the silver and bronze medals, respectively. Levchenko's success at 19 meant she became the event's youngest ever medallist in its history.

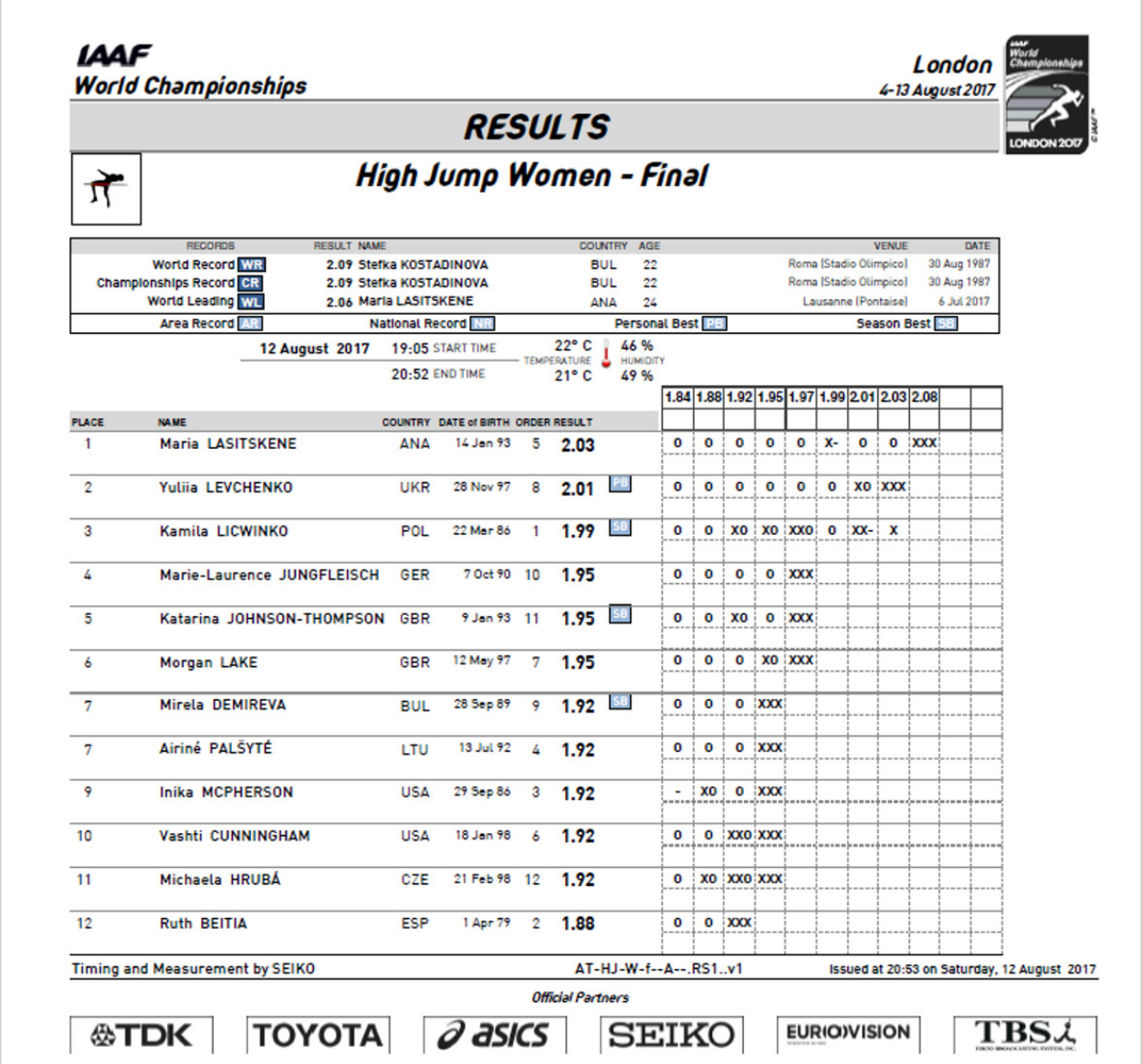

IAAF World Championships — London 4-13 August 2017

RESULTS

High Jump Women - Final

RECORDS	RESULT	NAME	COUNTRY	AGE	VENUE	DATE
World Record WR	2.09	Stefka KOSTADINOVA	BUL	22	Roma (Stadio Olimpico)	30 Aug 1987
Championships Record CR	2.09	Stefka KOSTADINOVA	BUL	22	Roma (Stadio Olimpico)	30 Aug 1987
World Leading WL	2.06	Maria LASITSKENE	ANA	24	Lausanne (Pontaise)	6 Jul 2017

Area Record AR | National Record NR | Personal Best PB | Season Best SB

12 August 2017 — 19:05 START TIME — 22° C TEMPERATURE — 46 % HUMIDITY
20:52 END TIME — 21° C — 49 %

PLACE	NAME	COUNTRY	DATE of BIRTH	ORDER	RESULT		1.84	1.88	1.92	1.95	1.97	1.99	2.01	2.03	2.08
1	Maria LASITSKENE	ANA	14 Jan 93	5	2.03		o	o	o	o	o	x-	o	o	xxx
2	Yuliia LEVCHENKO	UKR	28 Nov 97	8	2.01	PB	o	o	o	o	o	o	xo	xxx	
3	Kamila LICWINKO	POL	22 Mar 86	1	1.99	SB	o	o	xo	xo	xxo	o	xx-	x	
4	Marie-Laurence JUNGFLEISCH	GER	7 Oct 90	10	1.95		o	o	o	o	xxx				
5	Katarina JOHNSON-THOMPSON	GBR	9 Jan 93	11	1.95	SB	o	o	xo	o	xxx				
6	Morgan LAKE	GBR	12 May 97	7	1.95		o	o	o	xo	xxx				
7	Mirela DEMIREVA	BUL	28 Sep 89	9	1.92	SB	o	o	o	xxx					
7	Airiné PALŠYTĖ	LTU	13 Jul 92	4	1.92		o	o	o	xxx					
9	Inika MCPHERSON	USA	29 Sep 86	3	1.92		-	xo	o	xxx					
10	Vashti CUNNINGHAM	USA	18 Jan 98	6	1.92		o	o	xxo	xxx					
11	Michaela HRUBÁ	CZE	21 Feb 98	12	1.92		o	xo	xxo	xxx					
12	Ruth BEITIA	ESP	1 Apr 79	2	1.88		o	o	xxx						

Timing and Measurement by SEIKO — AT-HJ-W-f--A--.RS1..v1 — Issued at 20:53 on Saturday, 12 August 2017

Official Partners: TDK, TOYOTA, asics, SEIKO, EURIOVISION, TBS

METHODS

Unlike the qualification rounds, the landing mat for the high jump finals was positioned centrally (with respect to the field inside the running track) at the north side of the stadium. Four vantage locations for camera placement were identified and secured with each location having the capacity to accommodate at least one camera mounted on a tripod. Three of the locations were located on the north side of the stadium on broadcasting platforms whilst the remaining location was situated on the broadcasting balcony at the start of the home straight.

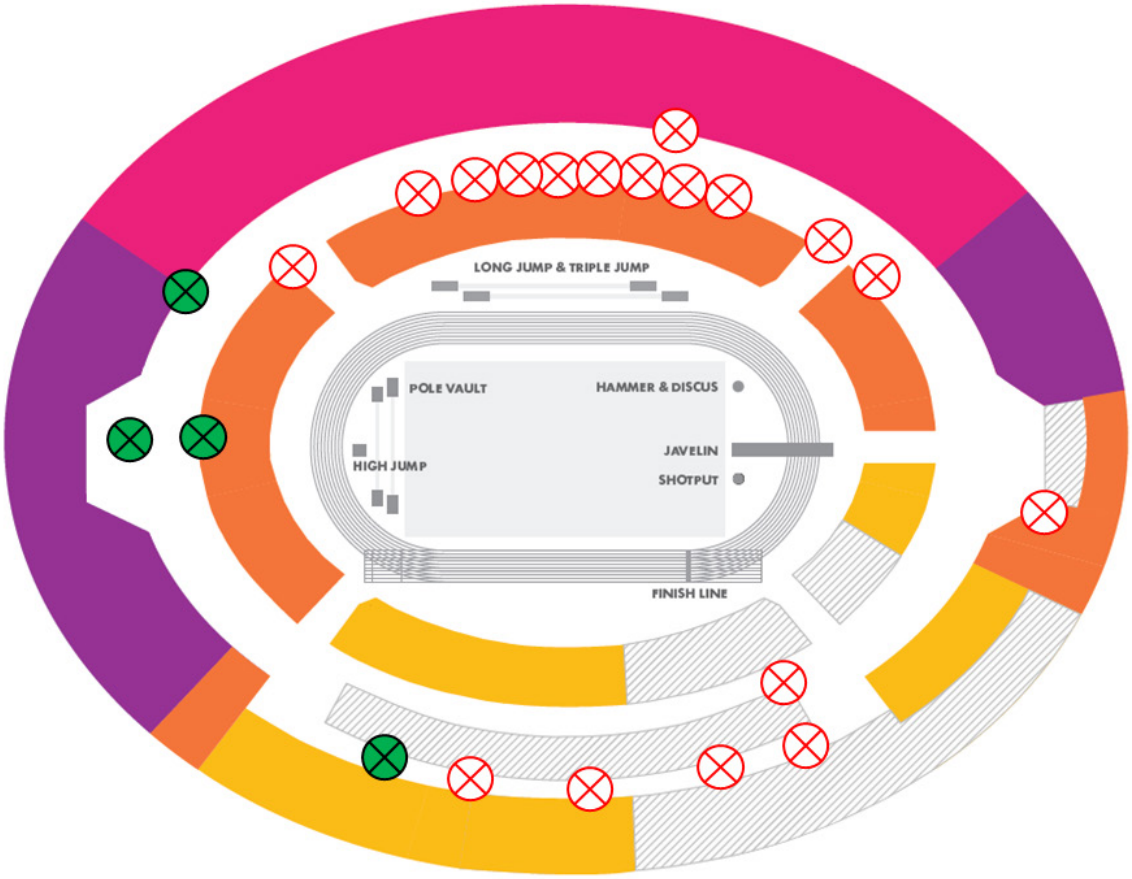

Figure 1. Camera locations for the women's high jump final (highlighted in green).

One standardised calibration procedure was conducted before and after the commencement of events on the evening of the final. Specifically, a rigid cuboid calibration frame was filmed on the high jump run-up / take-off area and repositioned multiple times over discrete predefined areas. This ensured an accurate defined volume for athletes who approached the uprights from both left and right directions. This approach produced a large number of non-coplanar control points per individual calibrated volume and facilitated the construction of a three-dimensional global coordinate system.

A total of five high-speed cameras were employed to record the action during the women's high jump final. Sony RX10 M3 cameras operating at 120 Hz (shutter speed: 1/1600; ISO: 1600; FHD: 1920x1080 px) were positioned strategically in pairs with their optical axes positioned to capture each athlete's attempt in both the frontal and sagittal planes. Separate camera pairings were utilised for athletes with left- and right-footed take-offs which enabled full-body motion capture to take place commencing three steps before take-off and ending when the athlete had landed.

Figure 2. The calibration frame was constructed and filmed before and after the competition.

The video files were imported into SIMI Motion (SIMI Motion version 9.2.2, Simi Reality Motion Systems GmbH, Germany) and the highest successful attempt for each athlete was manually digitised by a single experienced operator to obtain kinematic data. An event synchronisation technique (synchronisation of four critical instants) was applied through SIMI Motion to synchronise the two-dimensional coordinates from each camera involved in the recording. Digitising started 15 frames before the beginning of the first touchdown and ended 15 frames after the required sequence to provide padding during filtering. Each file was first digitised frame by frame and upon completion adjustments were made as necessary using the points over frame method, where each point (e.g. right knee joint) was tracked through the entire sequence. The Direct Linear Transformation (DLT) algorithm was used to reconstruct the three-dimensional (3D) coordinates from individual camera's x and y image coordinates. Reliability of the digitising process was estimated by repeated digitising of one full trial with an intervening period of 48 hours. The results showed minimal systematic and random errors and therefore confirmed the high reliability of the digitising process. De Leva's (1996) body segment parameter models were used to obtain data for the whole body centre of mass and for key body segments. A recursive second-order, low-pass Butterworth digital filter (zero phase-lag) was employed to filter the raw coordinate data. The cut-off frequencies were calculated using residual analysis. Where available, athletes' heights were obtained from 'Athletics 2017' (edited by Peter Matthews and published by the Association of Track and Field Statisticians) and online sources.

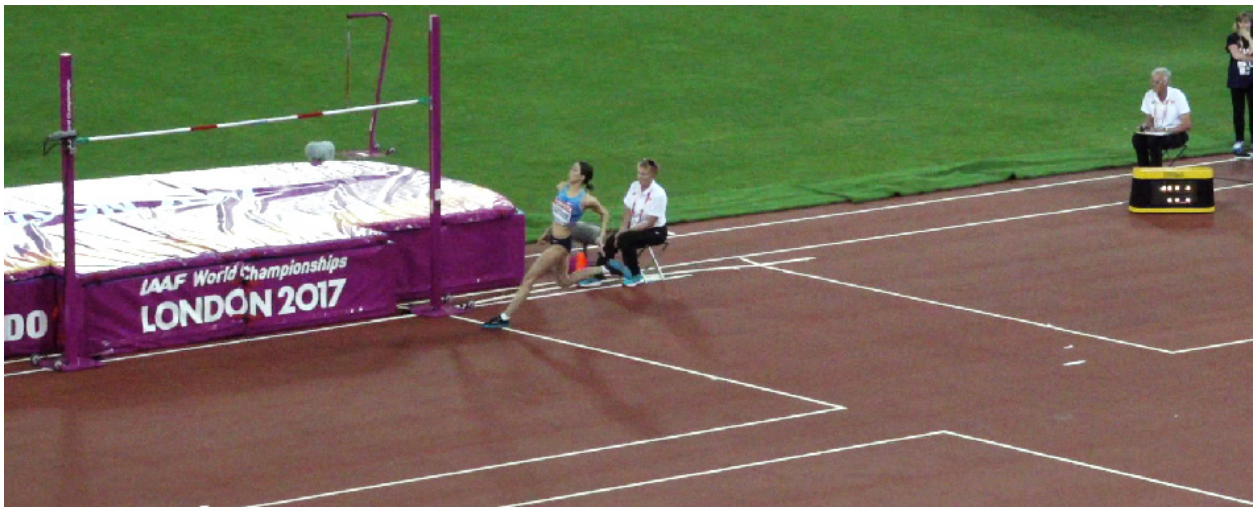

Figure 3. Action from the women's high jump final.

Each athlete's attempt was split into three consecutive parts:

1. *The Approach:* from the instant at which the athlete begins approaching the bar until the instant of touch-down for the take-off.
2. *The Take-off:* from the instant of touch-down (in the final contact) until the instant at which the take-off foot ends contact with the ground.
3. *The Flight/Bar Clearance:* from the instant of take-off until the instant of landing.

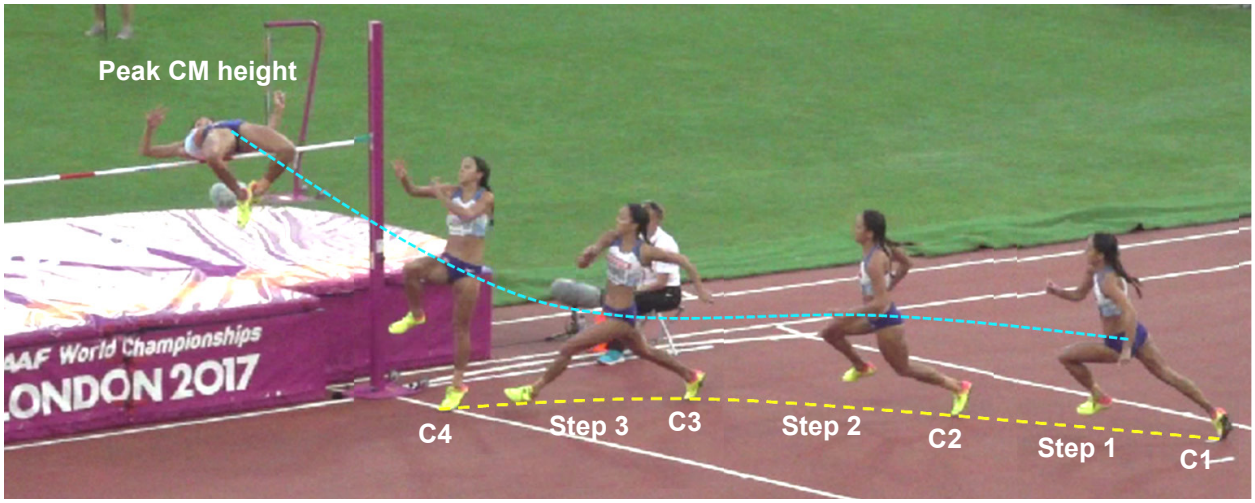

Figure 4. Key time-points at which the selected variables were obtained. C1-C4 denote foot contacts.

As the take-off conditions depend on the characteristics of the approach steps, the support and flight times, step lengths, centre of mass (CM) height, path of the centre of mass, angle of the run-up and horizontal / vertical velocities were computed throughout the last 3 steps of the athletes run-up. With regards to take-off, the contact time, distance from the bar, body segment

angles, take-off angle, horizontal/vertical velocities and location of the CM were computed. To complete the analysis, the peak height of the CM and location of the peak CM height with respect to the bar was obtained. In addition to an in-depth understanding of the characteristics of each finalist's best jump, the aforementioned parameters enabled the attempts to split into the following three partial heights:

1. *H1:* the height of the CM at the instant of touch-down (TD) during the final contact.
2. *H2:* the height of the CM at the instant of toe-off (TO) during the take-off phase.
3. *H3:* the peak vertical height of the CM during flight.

Table 1. Definitions of mechanical and performance variables.

Variable	Definition
CM height	The vertical height of the CM at various instances during the approach, take-off and flight.
∆ TO height (%)	The change in CM height (percentage of standing height) from TD to TO during the take-off phase.
Mean CM height	The mean height (% of standing height) of the CM at TD and TO throughout the approach (not including final TO).
% CM lowering	The percentage difference in CM height at TD between the penultimate and final foot contact.
Peak CM location	The anteroposterior distance of the CM from the bar at the instant of peak CM height.
Peak pelvis height	The maximum vertical height of the pelvis during flight.
PPH diff	The difference between peak pelvis height and the mark attained.
Path of run-up	The overhead representation of the path of the CM during the last three approach steps.
CM attack angle at TO 1-4	The angle between the peak CM position over the bar and the CM position at toe-off of each foot contact during the run-up (viewed overhead).
Step to bar angle at foot contacts 1-3	The angle between each respective foot contact relative to the bar.
Take-off distance (TOD)	The foot-tip distance (anteroposterior) from the bar at take-off.
Step length (SL)	The displacement between toe-off of consecutive foot contacts.
Contact time (CT)	The time spent in contact with the ground during each foot contact.
Flight time (FT)	The time spent airborne during each step of the approach.

Ratio (FT/CT)	The flight time divided by the subsequent contact time.
Vertical velocity (V_v)	The vertical velocity of the CM at various time instants.
Horizontal velocity (V_h)	The horizontal velocity (resultant of anteroposterior and mediolateral components) of the CM at various time instants.
Resultant velocity (V_r)	The resultant velocity of the CM at various time instants.
Ratio of velocity change ($\Delta V_v / \Delta V_h$)	The change in vertical velocity relative to the change in horizontal velocity during the take-off phase.
Velocity transfer	The change in vertical velocity (from TD to TO) relative to the horizontal velocity at TD during the take-off phase.
Take-off angle	The angle of the CM relative to the horizontal at the instant of take-off (calculated from take-off velocities).
Knee angle at TD/TO	The angle of the thigh relative to the shank at the instant of TD / TO during the penultimate or final foot contact. (180° = full extension)
Knee / Ankle lowest	The minimum angle of the knee and ankle during the take-off phase.
Ankle angle at TD/TO	The angle of the shank relative to the foot at the instant of TD / TO during take-off. (180° = full plantar flexion)
Knee flexion / extension duration	The time between maximum knee flexion and TD or TO during take-off.
Whole-body lean at TD/TO	The angle of the line between the CM and ankle joint (take-off leg) relative to the vertical at TD and TO during the take-off phase.
Trunk lean at TD	The angle of the trunk relative to the vertical at TD during the take-off phase.
Side-ways trunk lean at TD	The lean angle of the trunk (inward / outward) relative to the vertical at TD during the take-off phase. Positive values indicate inward lean.

Note: *CM = centre of mass.*

RESULTS

Table 2 below shows the highest clearance mark for each of the finalists and compares the mark to the season (2017) and personal best for each athlete.

Table 2. Best mark attained for each of the finalists expressed relative to their previous bests (before the London World Championships).

Athlete	Season's best (SB) (m)	Personal best (m)	Mark (m)	Difference from SB (%)
LASITSKENE	2.06	2.06	2.03	−1.46
LEVCHENKO	1.97	1.97	2.01	2.03
LICWINKO	1.98	2.02	1.99	0.51
JUNGFLEISCH	1.97	2.00	1.95	−1.02
JOHNSON-THOMPSON	1.95	1.98	1.95	0.00
LAKE	1.96	1.96	1.95	−0.51
DEMIREVA	1.92	1.97	1.92	0.00
PALŠTYÉ	2.01	2.01	1.92	−4.48
MCPHERSON	1.96	1.96	1.92	−2.04
CUNNINGHAM	1.99	1.99	1.92	−3.52
HRUBÁ	1.94	1.95	1.92	−1.03
BEITA	1.98	2.02	1.88	−5.05

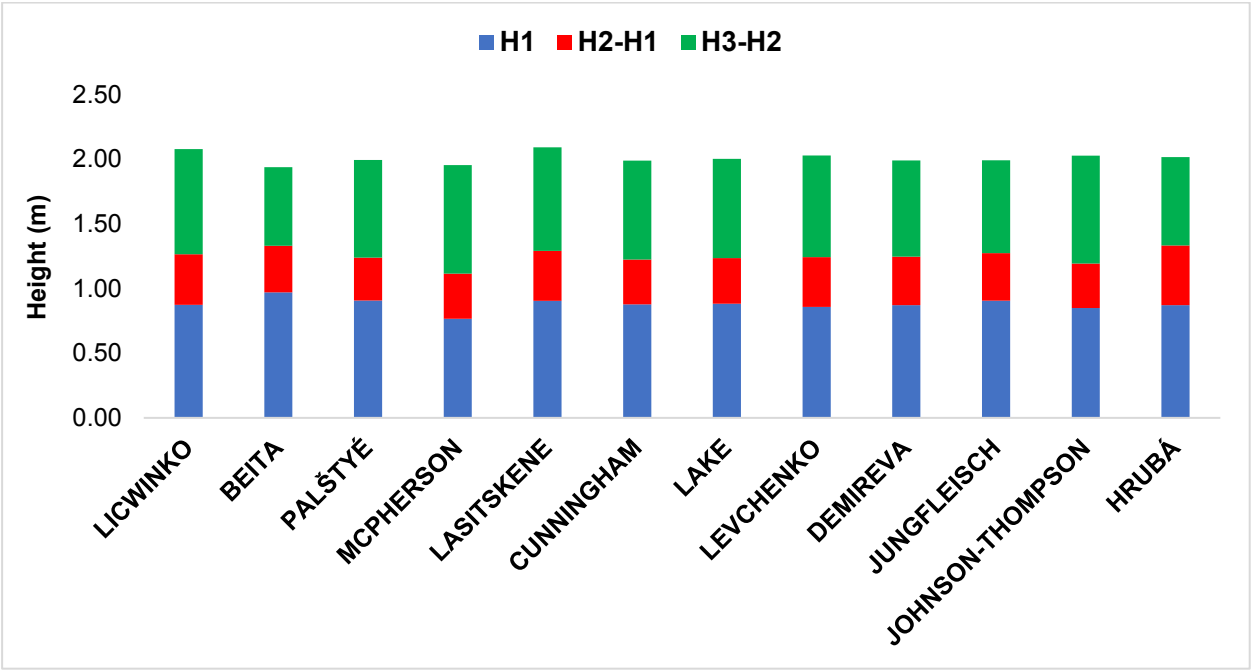

Figure 5. Partials heights of each athlete's CM during their best attempt.

Figure 5 on the previous page shows the partial heights of the CM during the take-off and flight phases of the jumps for each athlete. Table 3 below shows the individual and mean partial heights and also expresses these as a percentage of each athlete's standing height.

Table 3. Partial heights of the CM (in metres and relative to each athlete's stature) along with the peak CM location, peak pelvis height and PPH diff for each finalist.

Athlete	H1 (m)	H2 (m)	H3 (m)	H3 diff (m)	H1 (%)	H2 (%)	H3 (%)	Peak CM location (m)	Peak pelvis height (m)	PPH diff (m)
LASITSKENE	0.91	1.29	2.09	0.06	50.33	71.83	116.33	−0.10	2.21	0.18
LEVCHENKO	0.86	1.24	2.03	0.02	47.99	69.50	113.46	0.06	2.16	0.15
LICWINKO	0.88	1.27	2.08	0.09	47.81	69.23	113.66	−0.17	2.16	0.17
JUNGFLEISCH	0.91	1.28	1.99	0.04	50.11	70.44	110.17	0.05	2.09	0.14
JOHNSON-THOMPSON	0.85	1.19	2.03	0.08	46.45	65.25	110.93	−0.01	2.13	0.18
LAKE	0.88	1.24	2.01	0.05	49.06	68.72	111.39	0.06	2.09	0.14
DEMIREVA	0.87	1.25	1.99	0.07	48.44	69.33	110.17	−0.28	2.07	0.15
PALŠTYÉ	0.91	1.24	2.00	0.08	48.87	66.67	107.31	0.01	2.11	0.19
MCPHERSON	0.77	1.12	1.96	0.04	47.06	68.47	120.00	−0.14	2.05	0.13
CUNNINGHAM	0.88	1.23	1.99	0.07	47.51	66.27	107.62	−0.11	2.10	0.18
HRUBÁ	0.87	1.34	2.02	0.10	46.44	71.01	107.34	−0.03	2.13	0.21
BEITA	0.97	1.33	1.94	0.06	50.63	69.38	101.04	−0.06	2.07	0.19

***Note**: Minus values for peak CM location indicate peak CM beyond the bar.*

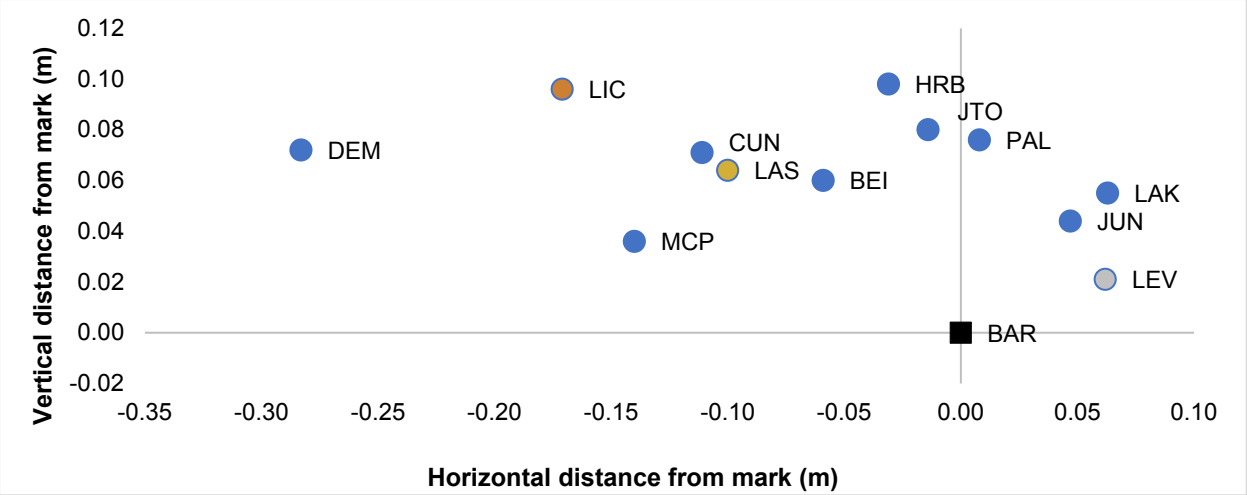

Figure 6. Scatterplot showing the distance of the CM (peak height) relative to the cleared mark in the vertical and horizontal directions for each finalist. Minus values on the horizontal scale indicate area beyond the bar.

Figure 6 on the previous page shows the horizontal and vertical distance of the peak CM height from the bar for each finalist. The contrasting bar clearance techniques of the medallists should be considered when interpreting Figure 6 and Table 3 since this varied between the finalists (Figure 7).

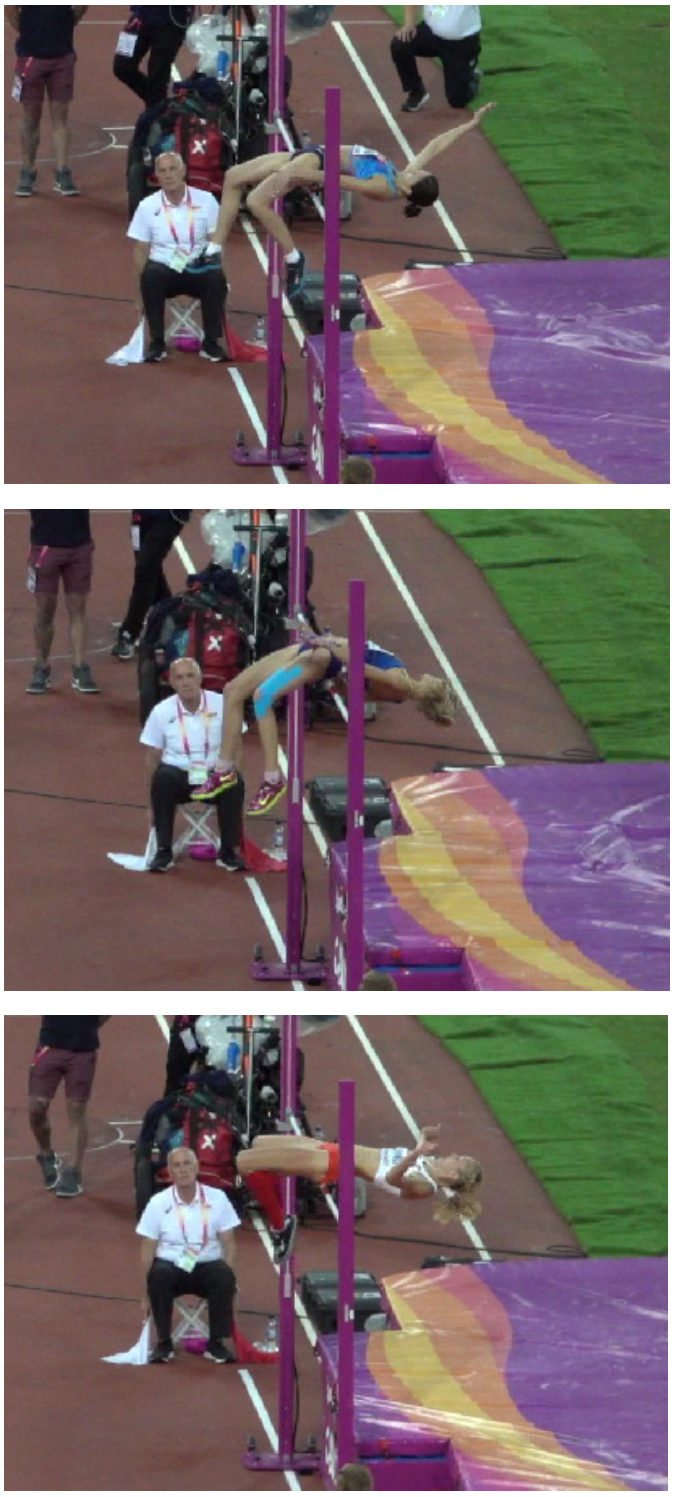

Figure 7. Contrasting bar clearance techniques of the medallists, with Lasitskene (top), Levchenko (middle) and Licwinko (bottom).

Table 4 below shows the height of the CM at the instant of touchdown during the second, third and fourth foot contacts along with the percentage change in height of the CM during the take-off phase. Table 4 also shows the mean height of the CM during each foot contact throughout the approach and the percentage lowering of the CM during the last step. Figure 8 on the next page visually depicts the CM lowering with the medallists being highlighted in their respective colours.

Table 4. The height (relative to stature) of the CM at contact two, three and four along with the change in height (% of stature) during the take-off phase, mean approach height (% stature) and the percentage lowering of the CM from penultimate to final TD (not relative to stature).

Athlete	Contact 2 TD (%)	Contact 3 TD (%)	Contact 4 TD (%)	Mean height (%)	CM lowering (%)	Δ TO height (%)
LASITSKENE	49.00	51.89	50.33	50.48	−3.00	21.50
LEVCHENKO	47.88	49.78	47.99	48.95	−3.59	21.51
LICWINKO	53.77	52.95	47.81	52.28	−9.70	21.42
JUNGFLEISCH	51.82	50.00	50.11	51.63	0.22	20.33
JOHNSON-THOMPSON	47.76	46.67	46.45	47.29	−0.47	18.80
LAKE	50.72	49.28	49.06	50.13	−0.45	19.67
DEMIREVA	52.39	51.78	48.44	51.98	−6.44	20.89
PALŠTYÉ	50.86	50.59	48.87	50.55	−3.40	17.80
MCPHERSON	48.83	47.73	47.06	50.59	−1.40	21.41
CUNNINGHAM	51.35	51.78	47.51	50.83	−8.25	18.76
HRUBÁ	46.54	47.77	46.44	47.83	−2.78	24.57
BEITA	51.35	51.51	50.63	51.59	−1.72	18.75

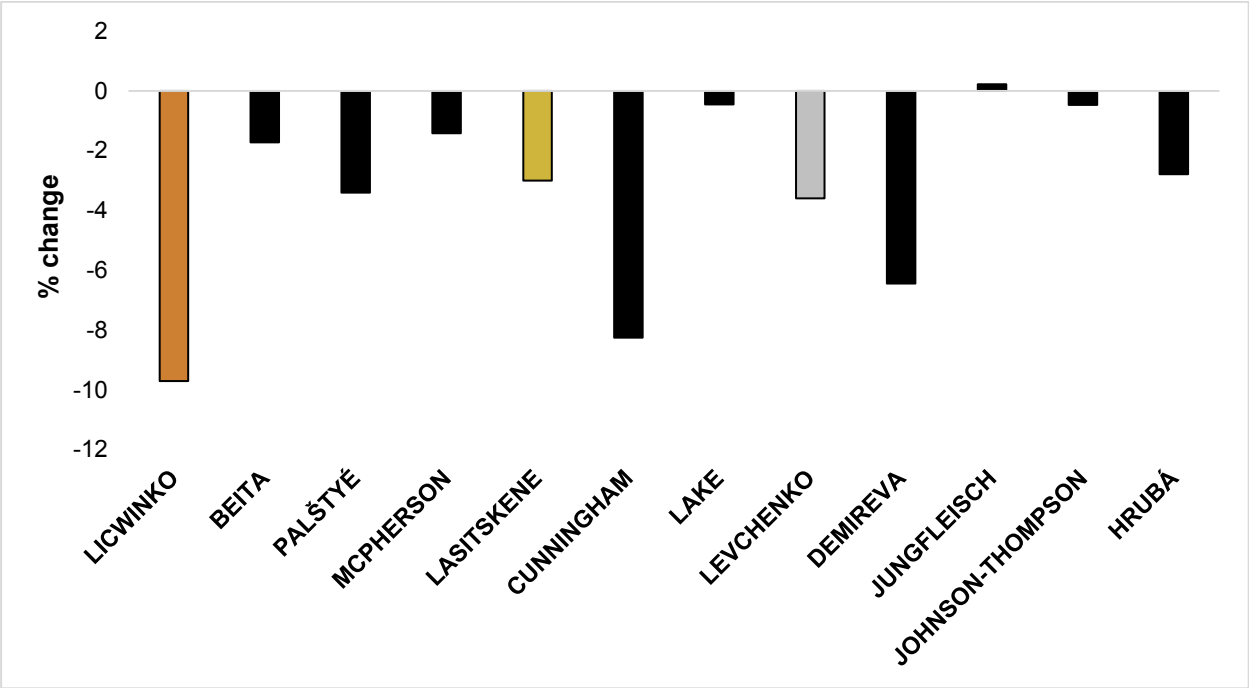

Figure 8. Percentage change in CM height during the last step for each of the finalists.

Figure 9 below shows the vertical position of the CM throughout the approach for the gold medallist.

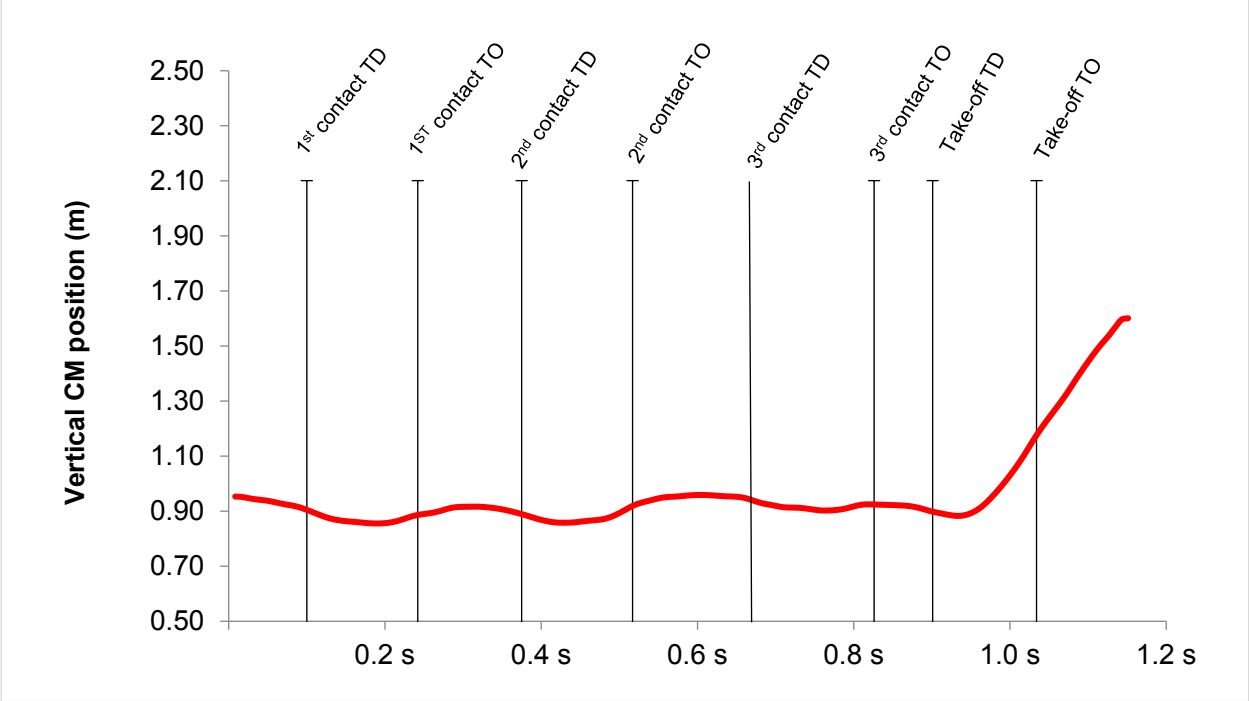

Figure 9. The vertical position of the CM during the approach for the gold medallist.

Table 5 on the next page shows the specific values for the horizontal velocity during each contact as well as the peak velocity during the approach. Figure 10 on the next page shows the horizontal velocity of each finalist during the second, third and fourth foot contacts during the approach.

Table 5. The horizontal velocity of the CM at TD during each foot contact (fourth contact = take-off) and at TO of contact four. The change (%) in horizontal velocity during take-off (from TD to TO) is also displayed.

Athlete	V_h 2nd contact TD (m/s)	V_h 3rd contact TD (m/s)	V_h 4th contact TD (m/s)	V_h 4th contact TO (m/s)	ΔV_h during take-off (%)
LASITSKENE	7.12	7.23	6.71	4.38	−34.72
LEVCHENKO	7.33	7.10	6.61	4.39	−33.59
LICWINKO	7.21	7.16	6.64	3.88	−41.57
JUNGFLEISCH	6.65	6.74	6.82	4.60	−32.55
JOHNSON-THOMPSON	6.93	7.08	6.64	3.77	−43.22
LAKE	7.13	7.41	6.99	4.41	−36.91
DEMIREVA	7.02	6.96	6.90	3.62	−47.54
PALŠTYÉ	7.07	6.69	6.51	3.74	−42.55
MCPHERSON	7.62	7.64	6.98	4.35	−37.68
CUNNINGHAM	6.99	6.90	6.56	3.49	−46.80
HRUBÁ	6.93	6.81	6.65	4.01	−39.70
BEITA	6.35	6.65	6.45	4.23	−34.42

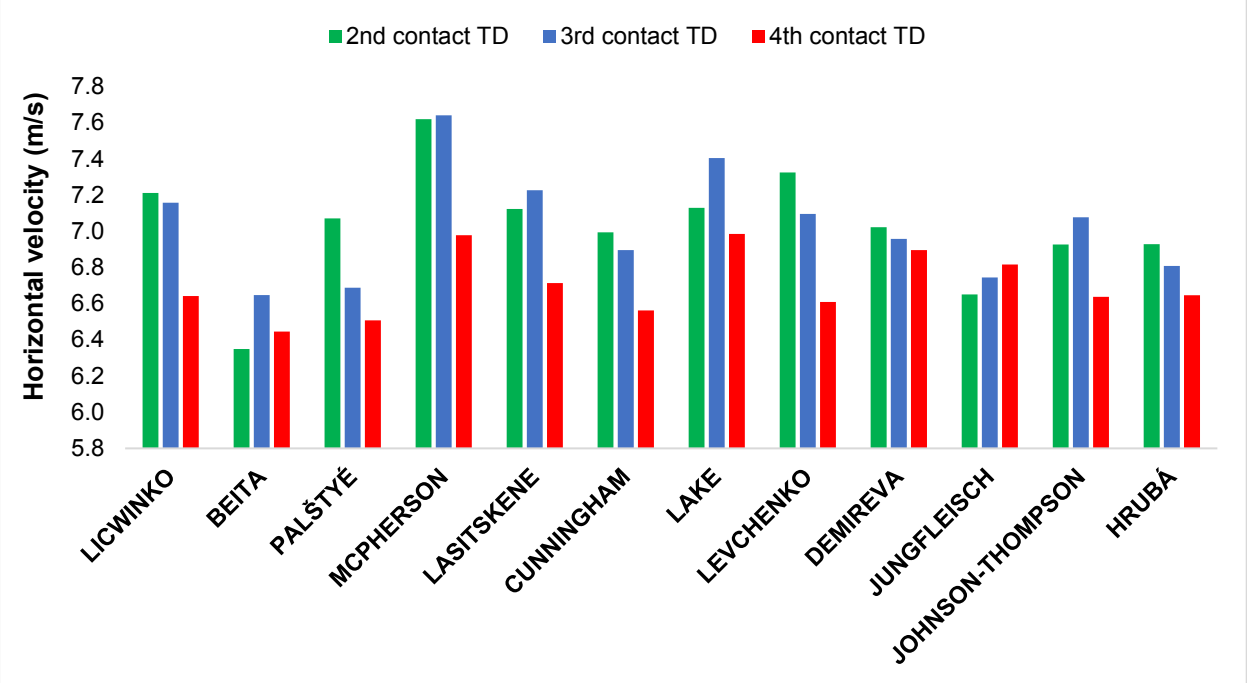

Figure 10. The horizontal velocity of each finalist at TD during the second, third and fourth (take-off) foot contacts.

Figure 11 below shows the rear foot position displayed by three of the finalists during the take-off phase.

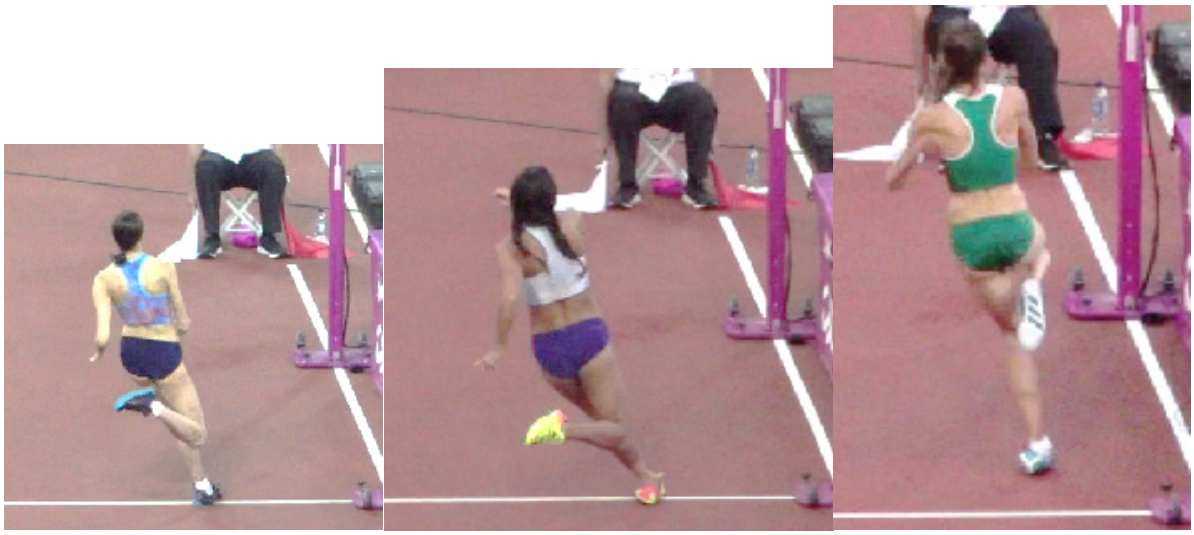

Figure 11. Contrasting rear foot position during take-off TD for three of the finalists.

Table 6 below shows the CM angle of attack at toe-off during the first, second, third and fourth (take-off) foot contacts whilst Figure 12 shows how these angles were constructed. The angles are smaller for athletes who move more parallel to the bar.

Table 6. CM attack angle at toe-off for the first, second, third and fourth foot contacts along with the percentage change in this angle from the first to the fourth foot contact.

Athlete	CM attack angle 1st TO (°)	CM attack angle 2nd TO (°)	CM attack angle 3rd TO (°)	CM attack angle 4th TO (°)	Δ 4-1 (%)
LASITSKENE	47.65	43.87	41.01	37.45	−21.41
LEVCHENKO	48.93	42.41	38.80	37.80	−22.75
LICWINKO	52.08	47.53	43.47	43.44	−16.59
JUNGFLEISCH	50.50	45.89	41.01	25.39	−49.72
JOHNSON-THOMPSON	48.43	42.81	37.50	35.66	−26.37
LAKE	50.98	45.78	42.57	41.70	−18.20
DEMIREVA	46.09	41.11	37.62	35.94	−22.02
PALŠTYÉ	53.30	48.38	44.70	41.55	−22.05
MCPHERSON	53.58	49.03	44.52	42.23	−21.18
CUNNINGHAM	47.01	42.60	36.32	41.77	−11.15
HRUBÁ	48.93	44.20	40.33	40.25	−17.74
BEITA	41.95	36.91	35.14	36.02	−14.14

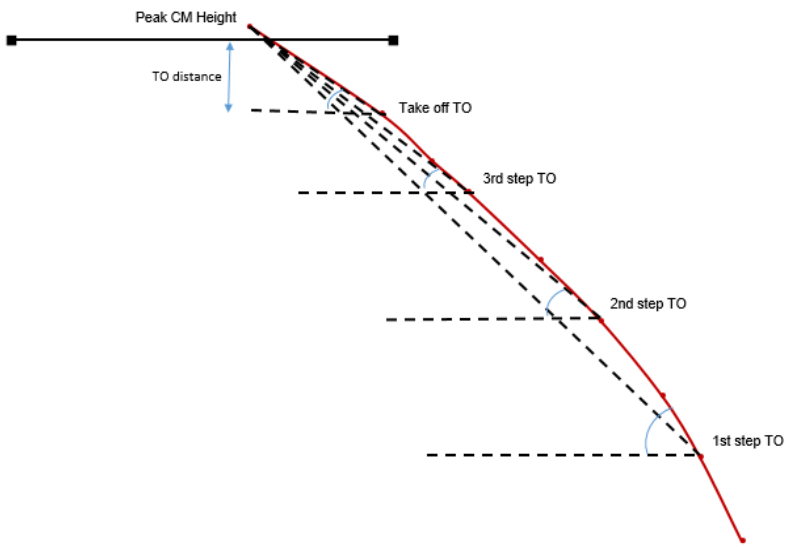

Figure 12. Overhead view of the CM path during the approach, take-off and airborne phase. Dashed lines depict the construction of the CM attack angles reported in Table 6.

Table 7 below shows the step-to-bar angles between each respective foot contact along with the percentage change from each angle to the next. Figure 13 shows how these angles were constructed. The angles are smaller for athletes who move more parallel to the bar.

Table 7. Step-to-bar angle between toe-off to toe-off of each respective foot contact along with the percentage change in these angles from one to the next (1-3 indicates the % change from the first to the final angle).

Athlete	SB angle 1-2nd TO (°)	SB angle 2-3rd TO (°)	SB angle 3rd-4th TO (°)	Δ 1-2 (%)	Δ 2-3 (%)	Δ 1-3 (%)
LASITSKENE	58.43	50.83	35.02	−13.01	−31.10	−40.07
LEVCHENKO	67.87	49.05	28.44	−27.73	−42.02	−58.10
LICWINKO	65.49	53.81	27.78	−17.83	−48.37	−57.58
JUNGFLEISCH	70.84	58.12	31.21	−17.96	−46.30	−55.94
JOHNSON-THOMPSON	62.44	56.79	22.90	−9.05	−59.68	−63.32
LAKE	65.59	52.31	33.91	−20.25	−35.17	−48.30
DEMIREVA	62.06	50.02	22.37	−19.40	−5.28	−63.95
PALŠTYÉ	70.88	56.20	34.65	−20.71	−38.35	−51.11
MCPHERSON	68.22	57.85	38.69	−15.20	−33.12	−43.29
CUNNINGHAM	59.67	52.86	30.55	−11.41	−42.21	−48.80
HRUBÁ	65.85	50.65	27.83	−23.08	−45.05	−57.74
BEITA	58.11	40.73	21.00	−29.91	−48.44	−63.86

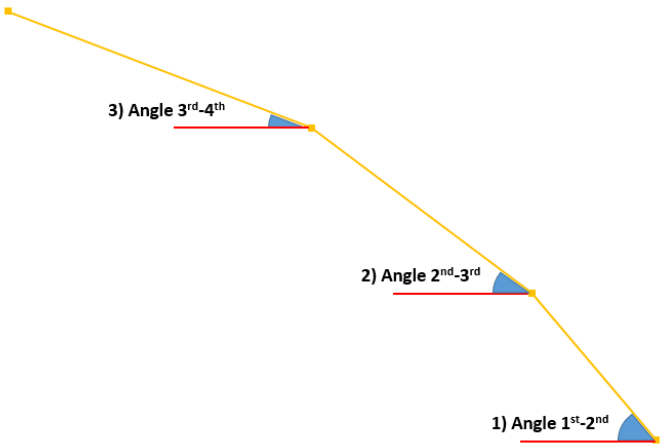

Figure 13. Schematic representation of the step-to-bar angle for each foot contact relative to the next.

Figure 14 below shows an overhead view of the CM path during the approach for each of the finalists relative to the bar (black solid line). Note: 'Right / left footers' are those who took off on the right and left legs, respectively.

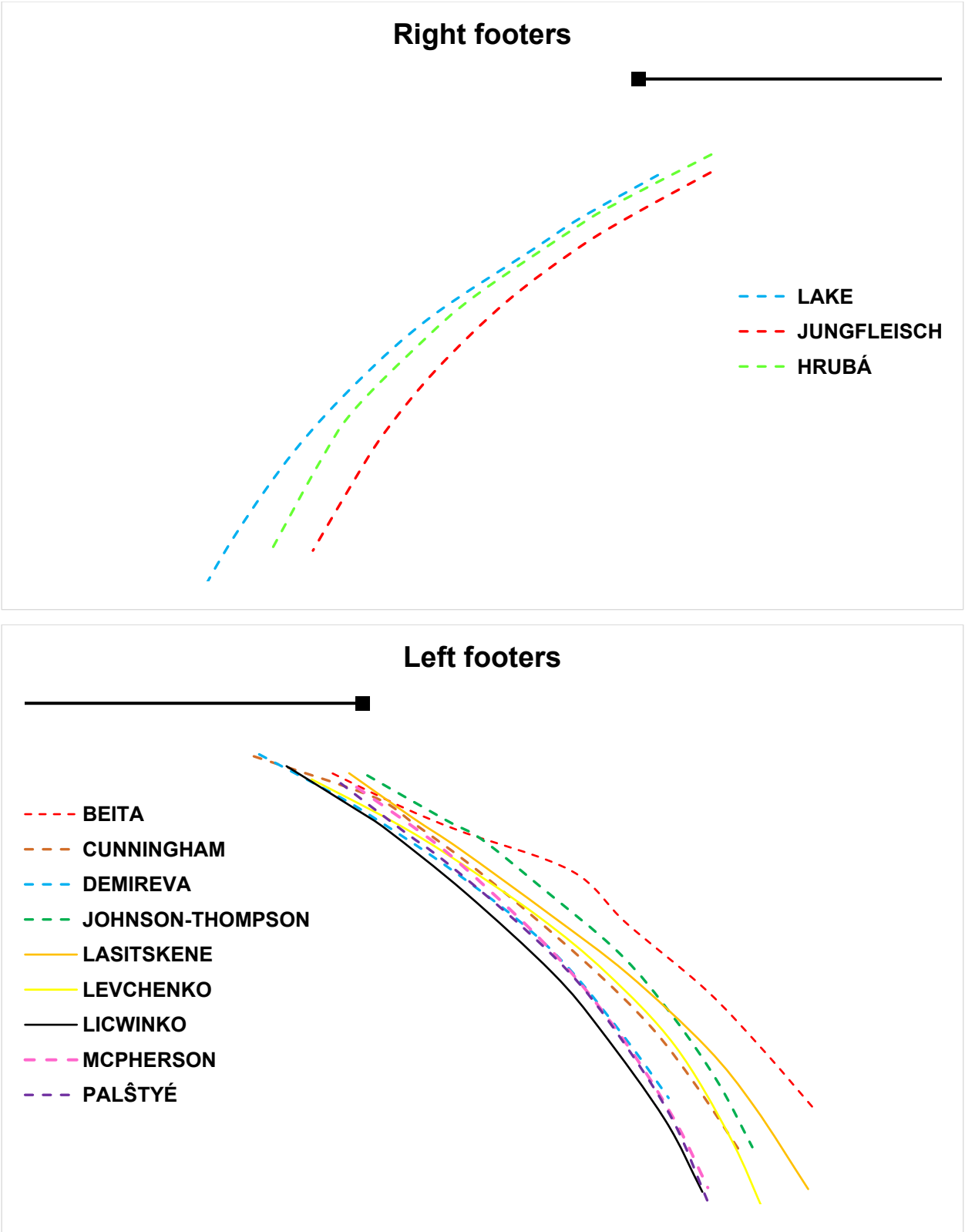

Figure 14. The overhead views of the paths of the CM during the approach and take-off for the finalists. Medallists are represented by solid lines.

Figure 15 below shows an overhead view of the whole body and foot paths during the approach, take-off and airborne phases for the three medallists.

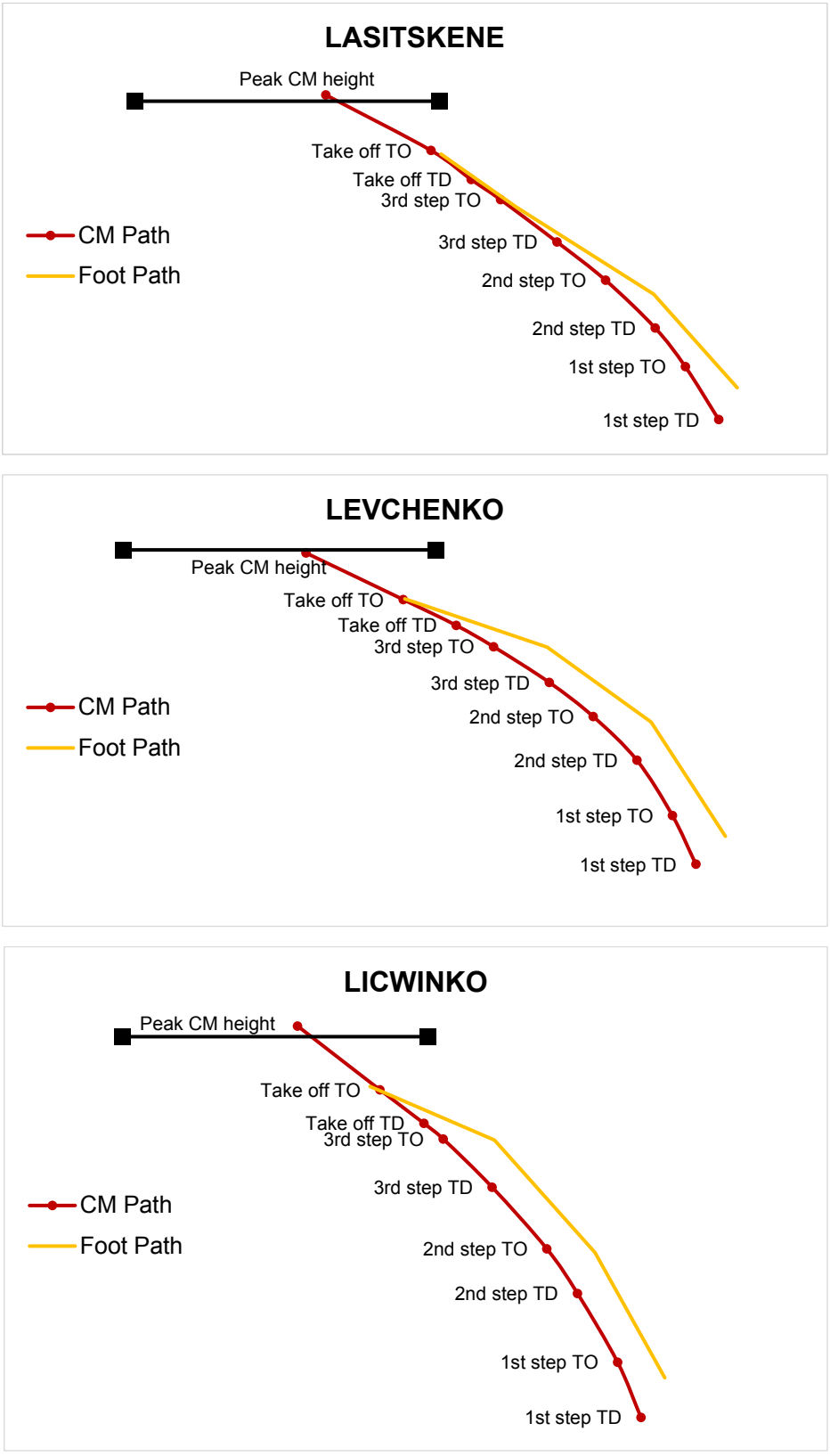

Figure 15. Overhead views of the CM and foot path during the approach, take-off and airborne phases for the three medallists.

Table 8 and Figure 16 below show the length of the last three approach steps along with the percentage change in absolute step length values (from step one to three) and duration of take-off for each of the finalists.

Table 8. The length of the last three approach steps along with the contact time of the take-off phase (CT) for the finalists. Step lengths are also expressed as a percentage of each athlete's standing height.

Athlete	1st step (m)	2nd step (m)	3rd step (m)	1st step (%)	2nd step (%)	3rd step (%)	Δ 3-1 %	Take-off CT (s)
LASITSKENE	2.09	2.13	1.75	115.87	118.38	97.48	−16.27	0.17
LEVCHENKO	2.51	2.02	2.06	140.28	112.95	115.31	−17.93	0.16
LICWINKO	2.20	2.22	1.84	120.24	121.41	100.36	−16.36	0.16
JUNGFLEISCH	1.66	2.00	1.95	91.54	110.35	107.49	17.47	0.14
JOHNSON-THOMPSON	1.95	1.96	1.80	106.39	106.85	98.17	−7.69	0.16
LAKE	2.26	2.13	2.01	125.38	118.38	111.85	−11.06	0.15
DEMIREVA	1.95	1.71	1.82	108.48	95.27	100.87	−6.67	0.17
PALŠTYÉ	2.02	1.94	1.82	108.46	104.36	97.77	−9.90	0.17
MCPHERSON	1.88	1.95	1.83	115.22	119.42	112.39	−2.66	0.15
CUNNINGHAM	1.99	2.25	1.89	107.47	121.85	102.31	−5.03	0.17
HRUBÁ	1.85	2.00	1.85	98.52	106.36	98.22	0.00	0.19
BEITA	1.96	1.92	1.77	102.02	99.86	92.28	−9.69	0.15

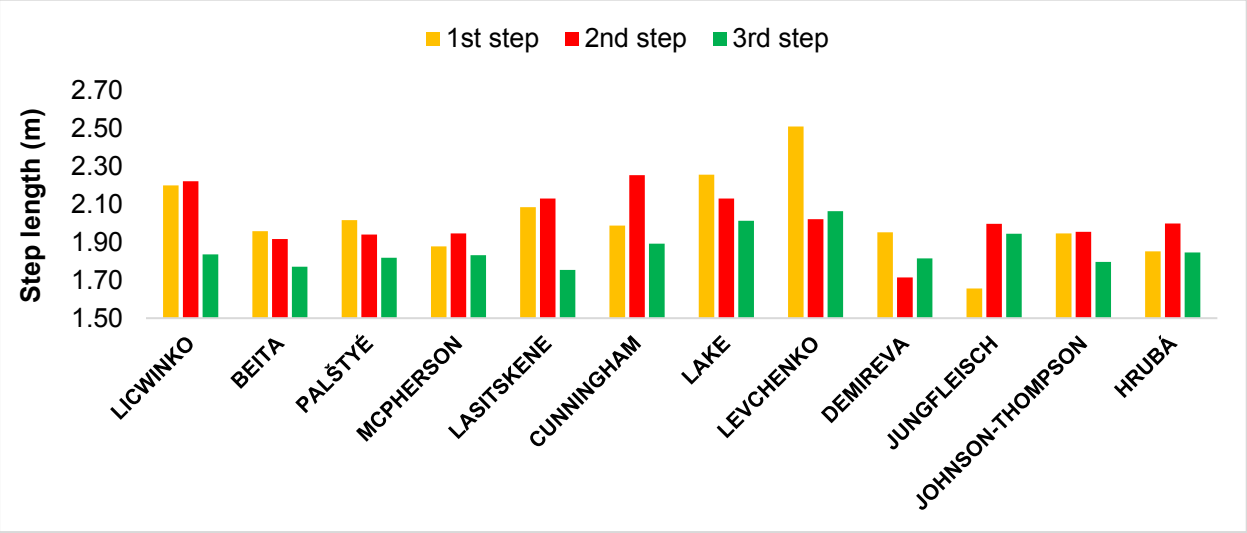

Figure 16. Length of the last three approach steps for each of the finalists.

Table 9 below shows the vertical and resultant velocities of the CM at key points during the take-off phase for each of the finalists along with various metrics showing the change in horizontal and vertical velocities with respect to each other. The take-off angle and take-off distance are also presented in the table with Figure 17 visually depicting the contrasting take-off distances adopted by two finalists.

Table 9. The vertical (V_v) and resultant (V_r) velocity values at TD and TO during the take-off phase along with the velocity transfer, take-off angle and take-off distances.

Athlete	V_v take-off TD (m/s)	V_v take-off TO (m/s)	Peak V_v (m/s)	V_r take-off TO (m/s)	Velocity transfer (%)	Ratio $\Delta V_v / V_h$	Take-off angle (°)	Take-off distance (m)
LASITSKENE	−0.77	4.13	4.31	6.02	73.03	−2.10	43	1.00
LEVCHENKO	−0.42	3.90	4.32	5.87	65.36	−1.95	41	0.97
LICWINKO	−0.41	4.11	4.39	5.65	68.07	−1.64	47	0.79
JUNGFLEISCH	−0.15	3.95	4.22	6.06	60.12	−1.85	41	1.14
JOHNSON-THOMPSON	−0.61	3.94	4.21	5.45	68.52	−1.59	46	0.84
LAKE	−0.37	4.09	4.25	6.01	63.81	−1.73	43	1.12
DEMIREVA	−0.73	4.07	4.12	5.45	69.57	−1.46	48	0.58
PALŠTYÉ	−0.43	3.69	3.94	5.25	63.29	−1.49	45	1.03
MCPHERSON	−0.38	4.16	4.25	6.02	65.10	−1.73	44	0.93
CUNNINGHAM	−0.67	4.00	4.25	5.31	71.19	−1.52	49	0.49
HRUBÁ	−0.24	3.94	4.03	5.62	62.89	−1.59	44	0.98
BEITA	−0.34	3.72	3.89	5.63	63.04	−1.83	41	0.97

Figure 17. The contrasting take-off distances of Jungfleisch (left) and Demireva (right).

Figure 18 below shows some relationships between key variables.

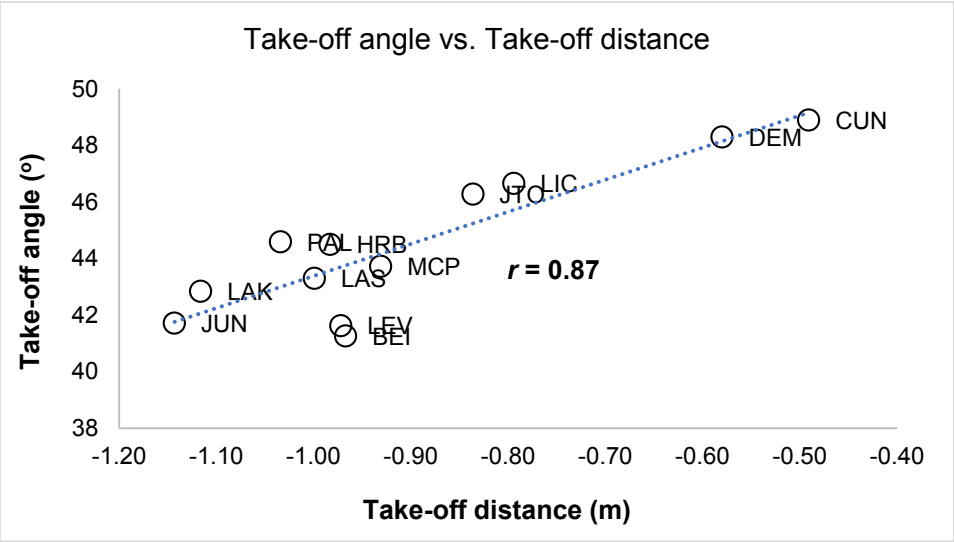

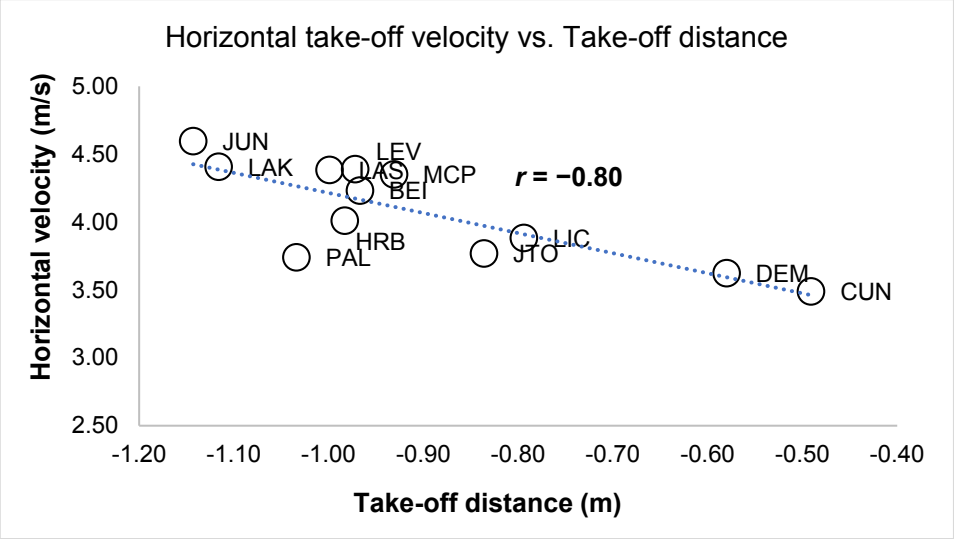

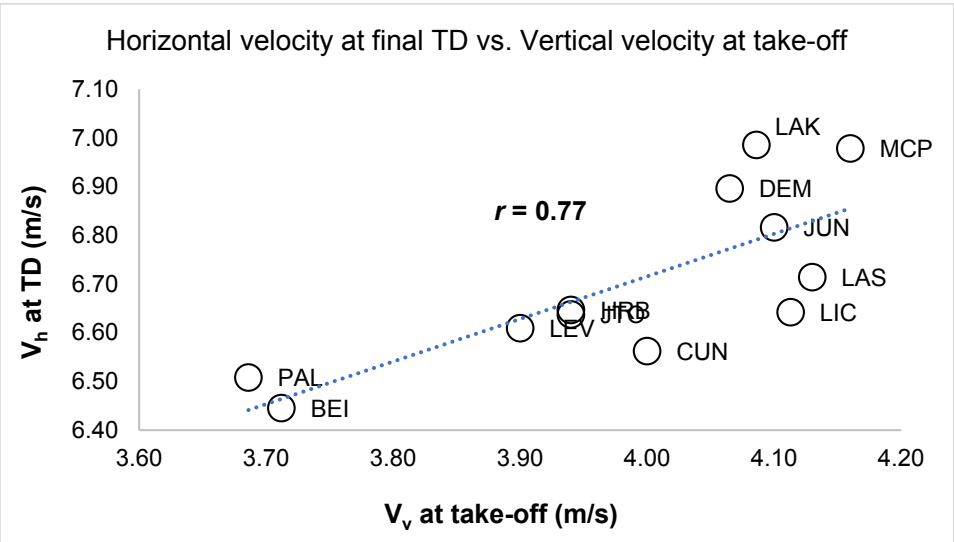

Figure 18. Scatterplots showing the relationships between key variables. *r* values indicate correlation coefficients.

Table 10 below shows the angles of the knee and ankle during the penultimate and final (take-off) foot contacts for each of the finalists.

Table 10. The knee angles at the instant of touchdown (TD) and toe-off (TO) during the penultimate foot contact for all finalists. Knee and ankle angles are also displayed at TD, TO and its lowest value during the final (take-off) contact.

	Penultimate		Take-off					
Athlete	**Knee angle TD (°)**	**Knee angle TO (°)**	**Knee TD (°)**	**Knee lowest (°)**	**Knee TO (°)**	**Ankle TD (°)**	**Ankle lowest (°)**	**Ankle TO (°)**
LASITSKENE	135	146	168	146	174	132	118	138
LEVCHENKO	136	141	156	127	173	123	102	134
LICWINKO	161	155	167	139	170	121	102	140
JUNGFLEISCH	136	150	164	137	168	133	105	136
JOHNSON-THOMPSON	144	146	159	148	168	138	105	144
LAKE	137	145	157	135	172	115	111	147
DEMIREVA	153	151	173	135	163	124	95	138
PALŠTYÉ	147	147	167	137	173	128	106	133
MCPHERSON	141	127	169	148	167	130	116	137
CUNNINGHAM	146	156	161	138	162	132	113	136
HRUBÁ	150	121	150	127	171	112	106	137
BEITA	140	152	169	146	174	133	109	139

Figure 19 below shows the magnitude of knee and ankle flexion during the take-off phase for each of the finalists.

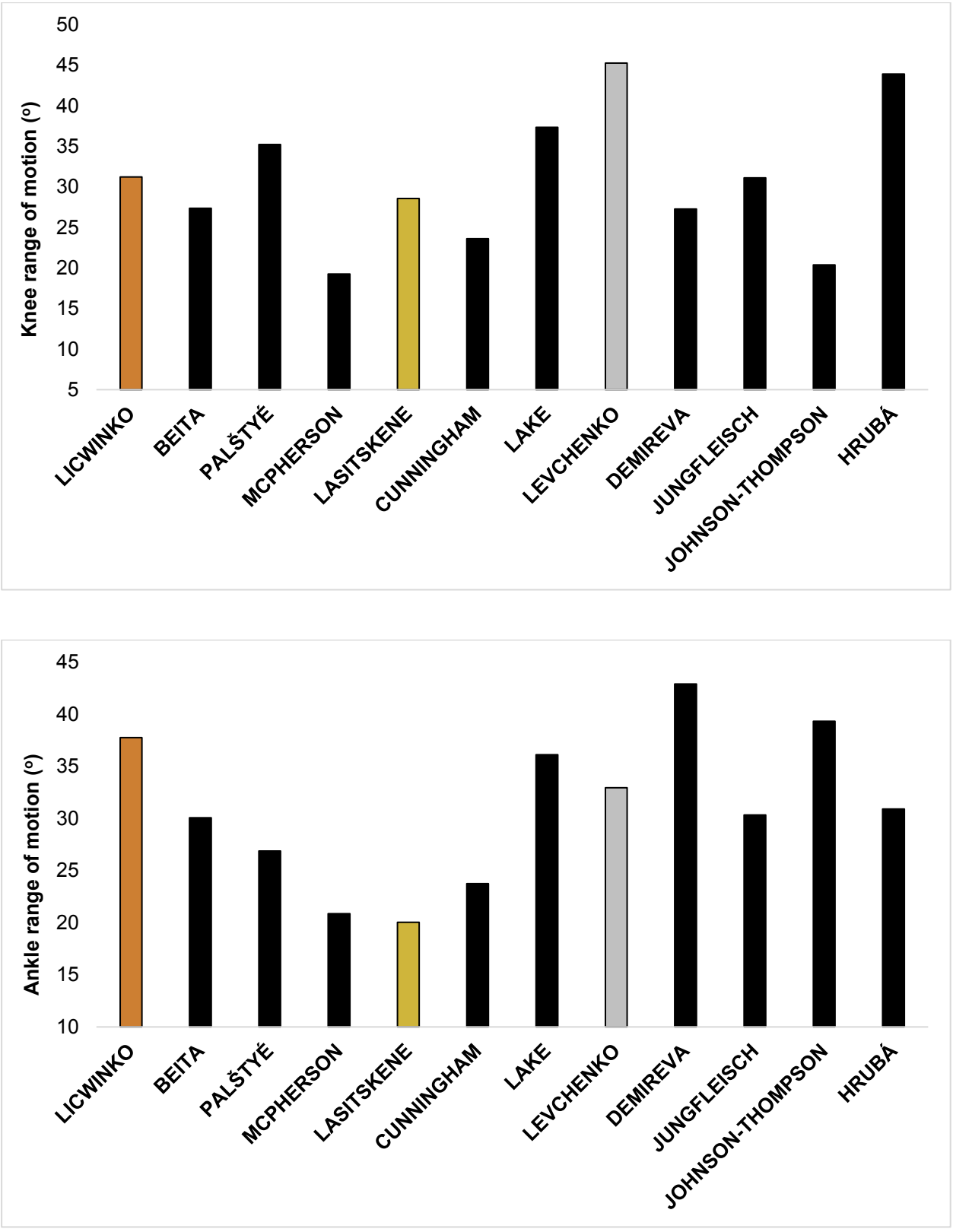

Figure 19. The top figure shows the range of motion between maximum knee flexion and the knee angle at take-off for each of the finalists. Bottom: Range of motion between maximum ankle flexion and the ankle angle at take-off for each of the finalists.

Figure 20 below provides an indication of the contact times and flight times for the final three approach steps. Note: contact 4 represents the duration of the take-off contact.

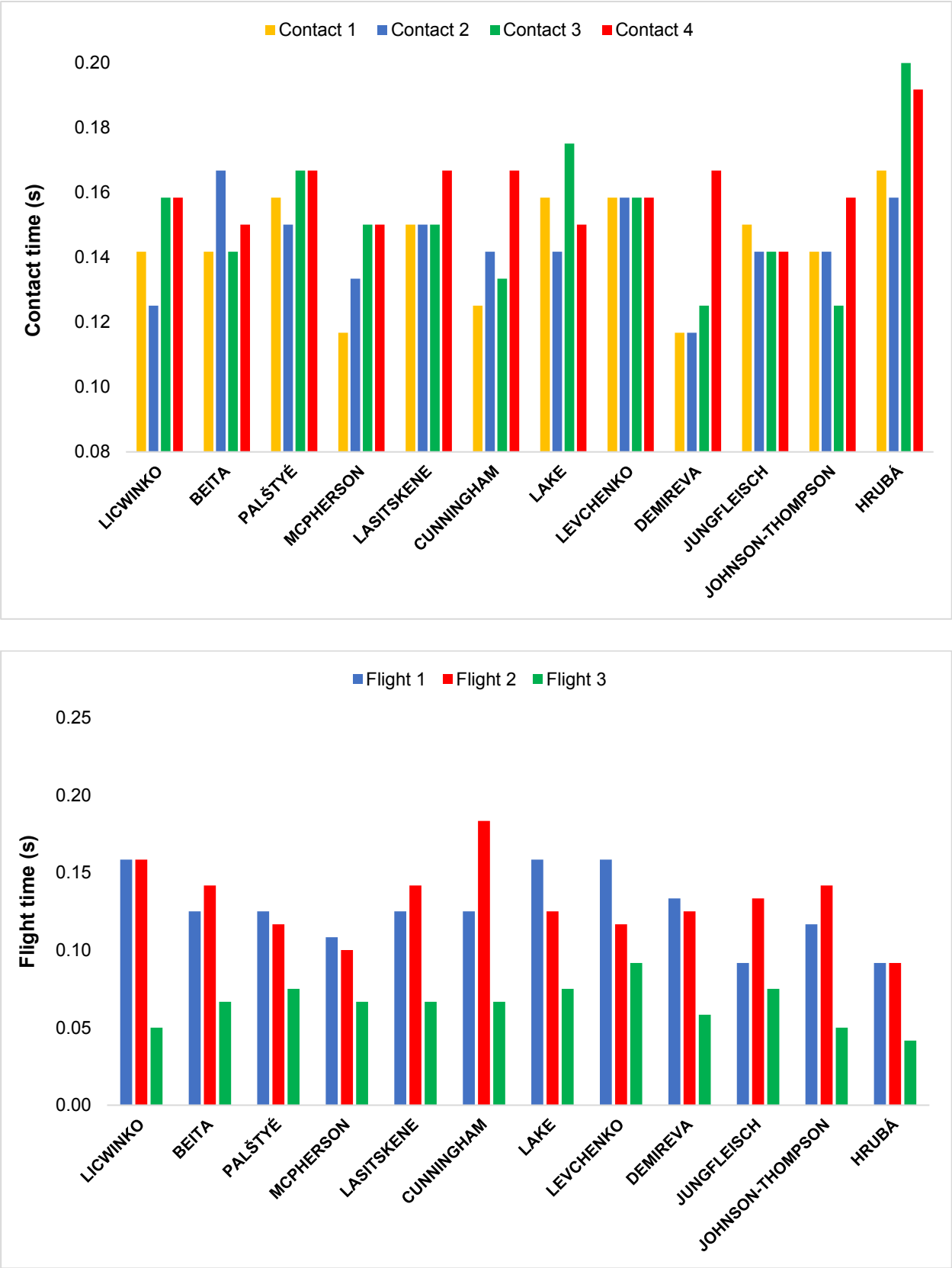

Figure 20. Top: Contact times for the final four ground contacts during the approach for each of the finalists. Bottom: Flight times for the final three steps before take-off (flight 3 precedes contact 4) for each of the finalists.

Figure 21 below shows (top) the ratio of flight time to contact time (flight time divided by the subsequent contact time) during the final step along with (bottom) the relationship between this ratio and the duration of knee flexion during the take-off phase.

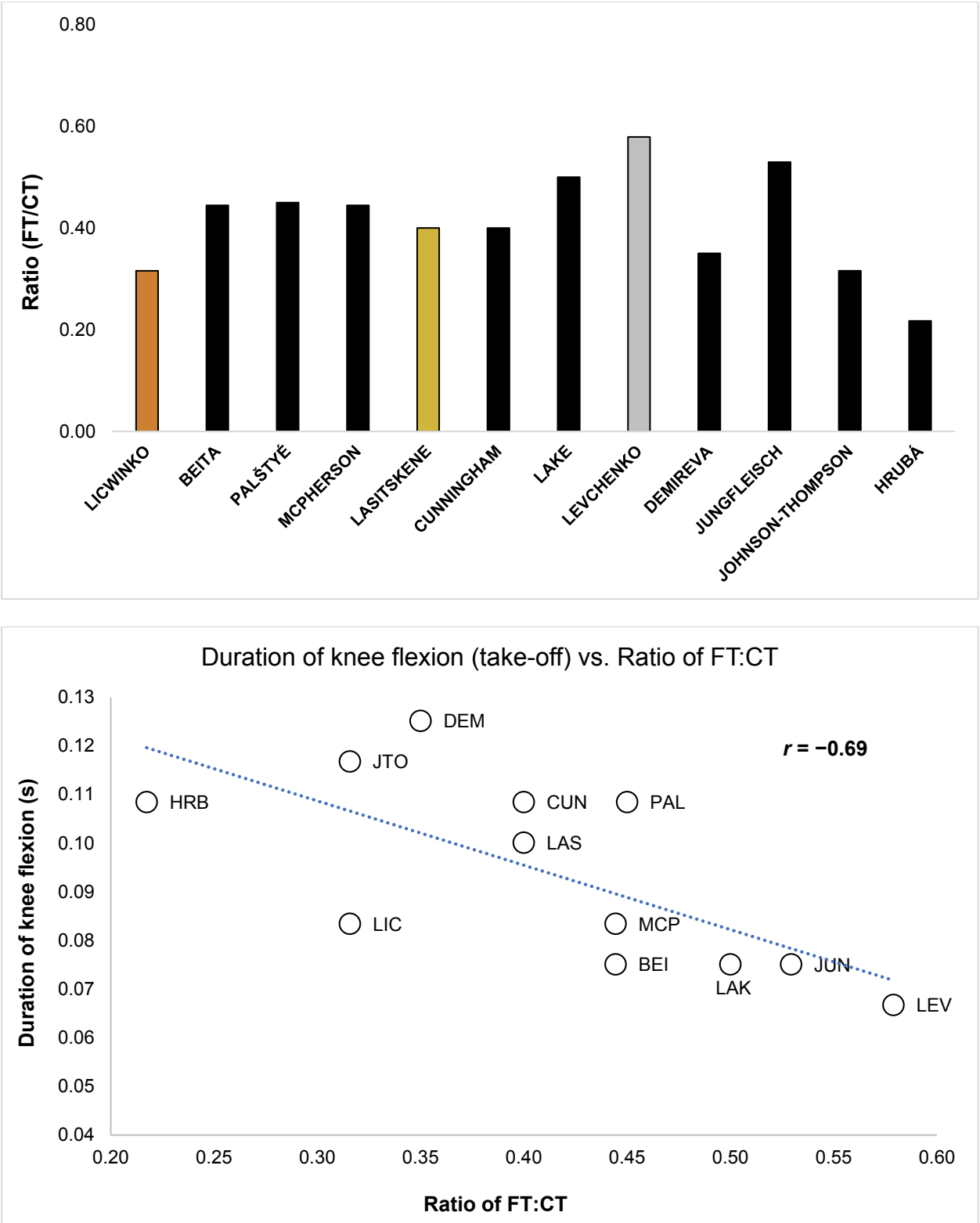

Figure 21. Top: Ratio of flight time to ground contact time during the final step. Bottom: relationship between the duration of knee flexion (during take-off) and the ratio of flight time to contact during the final step.

Table 11 and Figure 22 below show the time spent in knee flexion and extension during the penultimate and final foot contacts.

Table 11. The time spent in knee flexion and extension during the penultimate and final foot contacts.

	Penultimate contact		Final contact	
Athlete	**Flexion (s)**	**Extension (s)**	**Flexion (s)**	**Extension (s)**
LASITSKENE	0.08	0.08	0.10	0.07
LEVCHENKO	0.08	0.08	0.07	0.09
LICWINKO	0.09	0.07	0.08	0.08
JUNGFLEISCH	0.07	0.08	0.08	0.07
JOHNSON-THOMPSON	0.07	0.06	0.12	0.04
LAKE	0.07	0.10	0.08	0.08
DEMIREVA	0.06	0.07	0.13	0.04
PALŠTYÉ	0.09	0.08	0.11	0.06
MCPHERSON	0.08	0.07	0.08	0.07
CUNNINGHAM	0.06	0.08	0.11	0.06
HRUBÁ	0.12	0.08	0.11	0.08
BEITA	0.06	0.08	0.08	0.08

***Note**: Any differences in the duration of final contact from the Table 8 are a result of rounding differences.*

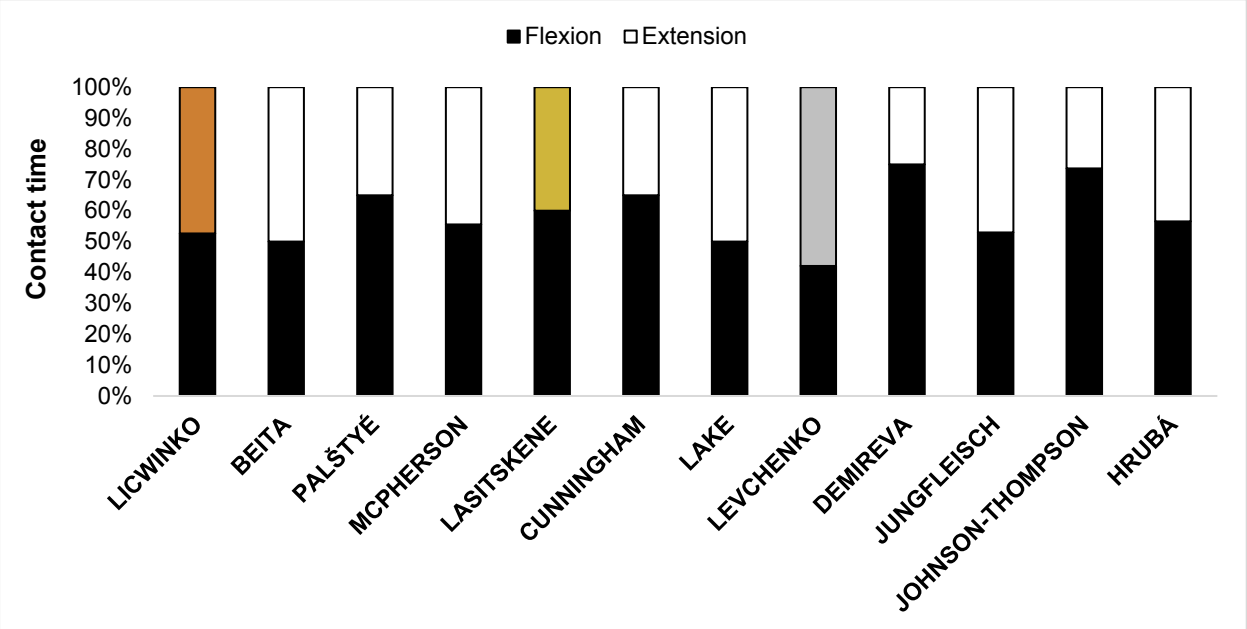

Figure 22. The percentage of time spent during knee flexion and extension during the final foot contact (take-off phase).

Table 12 below shows the whole-body and trunk lean at touchdown during the take-off phase along with the sideways lean of the trunk at TD. Figure 23 provides an example of body orientation at touchdown for one of the finalists.

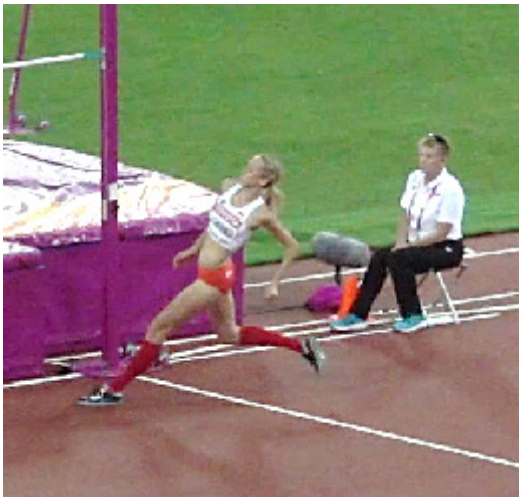

Figure 23. Example of body orientation at TD during the take-off phase for Licwinko.

Table 12. The whole-body lean at touchdown and toe-off during the take-off phase and the trunk lean at touchdown for each of the finalists.

Athlete	Whole-body lean (°)		Trunk lean at TD (°)	Side-ways trunk lean at TD (°)
	TD	TO *		
LASITSKENE	36	−8	14	7
LEVCHENKO	35	−8	8	8
LICWINKO	38	1	19	10
JUNGFLEISCH	33	−5	9	8
JOHNSON-THOMPSON	38	−4	16	7
LAKE	37	−4	13	9
DEMIREVA	37	0	16	9
PALŠTYÉ	34	−2	16	5
MCPHERSON	40	−2	13	5
CUNNINGHAM	38	0	21	6
HRUBÁ	40	−3	15	11
BEITA	31	−5	21	13

Note: ** negative value provides an indication of forward lean.*

COACH'S COMMENTARY

In terms of producing peak performance at the season's most important meeting it was Levchenko, Licwinko, Johnson-Thompson and Demireva who recorded their season's best in the final with Levchenko setting an all-time personal best. The other finalists recorded their season's best between seven weeks before two weeks after the championships.

The aim in the high jump event is for the athlete is to project the entire body over an increasingly raised horizontal fibreglass lath set on two narrow pegs without dislodging it. To be successful the athlete faces several challenges:

- Create sufficient horizontal momentum to pass from one side of the bar to the other
- Maximise the conversion of horizontal to vertical momentum to raise the body high enough to clear the bar
- Adjust the body position during the flight so as not to dislodge the bar

The final part of high jump approach comprising a series of chords is commonly referred to as a "curve". Adopting this approach run pattern is designed to enable the athlete to arrive at the point of take off with lateral and rearward displacement of the CM with respect to the final foot contact with a low centre of mass while minimising knee and hip flexion and speed loss. Such a position is intended to allow the athlete to develop to develop necessary tri-axial angular momentum during the actual take-off.

Biomechanically the high jump is a complex event. Uniquely when compared to the other three jump events in athletics, Dapena (2006) reported that an effective take off can be produced over a wide time frame ranging from 0.14 seconds (Howard) to 0.21 seconds. Ritzdorf (1989) reported take-off times for current world record holder Kostadinova of between 0.125 and 0.14 seconds. In London this time frame ranged from 0.14 seconds to 0.19 seconds.

Additionally the athlete has the freedom to approach the take-off point at an angle and speed of their choosing and select a take-off point relative to the bar in order to best generate the forces, vectors and rotations necessary for successful performance. There was some noted commonality. All athletes used a "curve" in the last three strides of the approach, displayed sideways lean away from the bar, had their shortest flight time between the penultimate and plant contacts and all (except Beita) employed a heel first plant, the recorded data also illustrated the great diversity in technical application between athletes.

- There was a large range of final approach run angles (step-to-bar) from 21.0 degrees (Beita) to 38.7 degrees (McPherson).
- Approach run angle change during the last stride ranged from sixteen degrees (Lasitskene) to thirty four degrees (Johnson-Thompson).

- Take-off distance from the bar ranged from 0.49 m (Cunningham) to 1.14 m (Jungfleisch).
- Sideways trunk lean at plant ranged from 5 degrees (Palsyte and McPherson) to 13 degrees (Beita).
- In the last two steps of the approach, ten athletes used a long/short pattern, with Levchenko and Demireva adopting a short/long stride pattern (Table 8).
- One stride before plant, six athletes touched down ball of foot first, one athlete used a full foot contact the remaining five used a heel contact (determined visually from video footage).
- All the athletes except Jungfleisch were slowing down into the take-off contact (Figure 10).
- As with the men there was variety in take-off arm actions. Six athletes employed a bar-side single arm lead. Of the six using a double arm shift, four brought both arms forward during the penultimate stride with the other two holding back their bar-side arm during the penultimate stride.
- All athletes except Jungfleisch lowered their CM during the last step (Table 4).
- Six athletes employed a tightly folded free knee. Five athletes employed an “open knee” free leg swing with Hrubá (who scraped the ground with her swinging foot) taking longer to complete the take-off (0.19 seconds) than all the other finalists.
- CM high point of the ranged from 28 centimetres beyond Demireva to 6 centimetres in front of the bar (Lake and Levchenko) with most jumpers CM high point being beyond the bar.

In a similar manner to her fellow ANA athlete Lysenko, Lasitskene made the smallest angle (step-to-bar) changes in the final strides of her approach run. Despite a high level of negative vertical velocity into plant, her stiff take-off was typified by short ranges of knee and ankle motion and good foot stability. She was able to lift her CM to 2.09 m. Like Levchenko, she ended the take-off with a large degree of forward/inward lean. Using one of the highest final step-to bar angles (35 degrees) she reached her high point some 10 centimetres past the bar adopting a flat layout position.

In the final two strides of her approach, Levchenko made angle changes of twenty degrees and seemed to have difficulty maintaining balance raising her bar-side arm high and to the side before her arm shift. With minimal rearwards trunk lean, her take-off was noteworthy for her ability move quickly through the eccentric phase of the plant contact and worked both knee and ankle concentrically over a large range of motion to record a take-off time of 0.16 seconds. Following take-off, she moved her CM moved laterally with the high point being 6 centimetres in front of the bar. Interestingly, she was able to demonstrate an efficient “layout position” with her CM (2.03 m) only 2 centimetres above the bar in achieving a new personal best.

Following a large change to her approach angle in the final stride (26 degrees), Licwinko entered

the take-off contact with some of the greatest rear/inward whole body and trunk lean and was able to leave the ground with her CM almost directly over her take-off foot. Despite employing an open knee swing she was able to move quickly through the eccentric phase of the take-off contact and record a take-off time of 0.16 seconds. Post take-off she moved significantly towards the bar ending up some 19 centimetres past the bar. Clearing 1.99 m she was unable to adopt an efficient layout with her CM passing 9 centimetres above the bar.

All three medallists utilised a double arm action.

The women used a narrower range of approach angles than the men. The fastest athlete (McPherson) planted at the highest angle to the bar at 39 degrees while the slowest (Beitá) had the narrowest final angle of approach at 21 degrees. With the exception of Levchenko, the range of approach angle changes among the finalists in the second step before take-off was 6-15 degrees (a similar range was noted for the men). As with the men, all the finalists made a larger angle change into the final stride.

In comparison with the men, the women tended to have less whole body and trunk rearward lean although inward lean appears similar. The women also tended to possess more forward and inward lean at the end of the take off than the men. This is consistent with the need for female high jumpers to acquire more angular momentum than male high jumpers. As women raise their CM less than the men, they reach the peak of their jump more quickly and as a consequence need to rotate at a faster rate. Considering the reported changes in whole body lean (inward and backwards) and the small degrees of inward lean (Table 12), coaches may wish to consider the most desirable ratio between transverse and frontal axes rotation to adopt during take-off.

To harness and maximise the generation and transmission of forces during the take-off, joint stiffness and stability in the take-off leg at both knee and ankle is desirable. In this regard over pronation in the plant is undesirable. Two women (Demireva and Johnson-Thompson) displayed large degrees of over pronation at take-off (determined visually from the high-speed video footage). Both athletes made large changes of direction in the final step of the approach (28-34 degrees) and planted at a narrow angle to the bar (<23 degrees) with noticeable negative vertical velocity. Both athletes also recorded a long eccentric phase during the take-off contact. Palšytė with a long eccentric phase during take-off also displayed noticeable pronation at plant. When coaching females, coaches may wish to consider the potential effects of the above combination of factors (particularly the amount of angle change per step, final direction into plant, negative vertical velocity and duration of eccentric component during the plant contact) when building a technical model.

Factors such as the ability to develop vertical momentum are critical to the performance of the event. The highest recorded CM's were achieved by the medallists along with Johnson-

Thompson. The medallists were all able to raise their CM by a similar amount (79-81 centimetres) with the fastest, and also the shortest athlete, McPherson able to raise her COM the most (86 centimetres) with Johnson-Thompson recording 84 centimetres.

There are noticeable gender differences. Women had typically lower take-off angles than the men typically around 44 degrees, some four degrees on average less than the men. Women also displayed slower final approach speeds than the men and the women tend to take-off closer to the bar. The data in Figure 18 (i) noted that the faster jumpers tended to take-off off further from the bar. This is sensible in order to give the athlete time to raise the CM and rotate the body into a supine position above the bar. Figure 18 (ii) suggests a tendency for athletes who can only generate a lower take of angle to take off further from the bar. Again this makes sense to prevent the athlete dislodging the bar during their ascent. There were some indications in Figure 18 (iii) that high rates of vertical momentum can be developed following a fast entry into take-off. Two successful examples were made by Lake and McPherson.

As with the men the variety of techniques on display confirm the fact, noted in previous studies that it is possible to adopt a variety of technical interpretations and still be successful. The challenge for the coach is to develop the technique that bests suits the physical makeup of their athlete.

CONTRIBUTORS

Dr Gareth Nicholson is a Senior Lecturer in Sport and Exercise Biomechanics at Leeds Beckett University and is Course Leader for the MSc Sport & Exercise Biomechanics pathway. Gareth has First Class Honours in BSc Sport and Exercise Science as well as an MSc in Sport & Exercise Science and a PhD from Leeds Beckett University. Gareth's research interests are in the measurement and development of strength and power. Gareth currently supervises a range of health and performance-related research projects.

Dr Athanassios Bissas is the Head of the Biomechanics Department in the Carnegie School of Sport at Leeds Beckett University. His research includes a range of topics but his main expertise is in the areas of biomechanics of sprint running, neuromuscular adaptations to resistance training, and measurement and evaluation of strength and power. Dr Bissas has supervised a vast range of research projects whilst having a number of successful completions at PhD level. Together with his team he has produced over 100 research outputs and he is actively involved in research projects with institutions across Europe.

A retired Head of Physical Education, Denis Doyle is an IAAF Level Five Elite Jumps coach and holds UKA Level Four Performance Coach. He has coached for 49 years across all sectors of the sport and has experience as a team manager for Great Britain and England and as a coach with British, Irish and Indian teams at four Olympics and six World Championships. His personal coaching record includes guiding over thirty five athletes from several nations to international success, five at Olympic level, with ten of them setting national senior and age group records. He is currently coach to 2nd world ranked U20 high jumper Tom Gale.